Remote-sensing monitoring of desertification using ASTER and ENVISAT ASAR: case study at semi-arid area of Vietnam

Hoang Viet Anh, Meredith Williams, David Manning

School of Civil Engineering and Geosciences
University of Newcastle upon Tyne, UK
v.a.hoang@ncl.ac.uk

Abstract

Mapping desertification in semi-arid and sub-humid region is difficult due to cloud cover data-unavailability. In this study, the potential of the Advanced Spaceborne Thermal Emission and Reflection Radiometer (ASTER) and ENVISAT ASAR for desertification mapping in semi-arid coastal area have been demonstrated. The project aims to develop a means of providing annually updated information at a range of spatial scales for local government and land use planners.

A desertification index was developed based on three parameters extracted from remote sensing data: land surface temperature (LST), vegetation index, and soil moisture. LST and vegetation index was extracted from ASTER thermal and VNIR band respectively. Soil moisture was estimated from the backscatter differences between wet and dry season ($\sigma_{wet} - \sigma_{dry}$). The result showed that vegetation index and LST are strongly related to moisture stress and can explain the variation of desertification level. Soil moisture estimation from delta backscatter ($\sigma_{wet} - \sigma_{dry}$) showed a strong relation with field measurements ($r^2 = 0.89$) for bare land and sparsely vegetated areas. When the vegetation density is higher (NDVI>0.5), the relation is weaker ($r^2 = 0.58$). The final step is to combine all 3 parameters into a angle desertification index.

INTRODUCTION

1.1 Background

Desertification is a form of land degradation in arid, semi-arid and dry sub-humid areas resulting from various factors, including climatic variations and human activities (UNCCD, Article 1). Desertification undermines the land's productivity and contributes to poverty. Prime resources - fertile topsoil, vegetation cover, and healthy crops - are the first victims of desertification. The people themselves begin to suffer when food and water supplies become threatened. In the worst cases, they endure famine, mass migration, and colossal economic losses. Over 250 million people are directly affected by desertification, and some one billion are at risk (UN, 2003).

Since the International Convention on Desertification of the United Nations that came into force in 1996 (UNCCD, 2004), the need to measure land degradation and desertification processes has substantially increased. The most obvious way to improve the availability and accuracy of desertification monitoring would be to employ remote sensing data, such as aerial photography and satellite imagery, which are design to survey ground condition over a large area (Grainger, 1990). A well-design remote sensing programme could in theory tell us how

large an area was decertified, and by carrying out regular surveys we could detect increase in the intensity and extent of degradation in different area.

If a frequent repetitive coverage with relatively low spatial resolution is desired one would certainly chose to use the AVHRR system available from the polar-orbiting satellites of the NOAA series. Based on NOAA imagery we can produce normalized vegetation index (NDVI) for the entire earth on a twice daily basic under cloud free conditions. Despise its low spatial resolution (1.1 km × 1.1 km), the data is so far one of the most widely used to analyze biomass changes at the global and regional scale (Tucker, 1980; Tucker, 1987). Alternatively, if looking for the highest spatial resolution available, even at the low repetition rates, one would chose one of the available Earth observation system. Since its came into operation in 1972, Landsat image have been successfully used to map the change of sand dune, denudation forming in West Africa (Dwivedi et al., 1993; Mering et al., 1987; Robinove et al., 1981). Merging with Radar data, Landsat imagery shows its ability to detect the change in desertification process at a more detail level (Rebillard et al., 1984).

Due to the tragedic crisis in Sahara Shale in 1970s which captured the public's attention, most of the desertification mapping in the early days was focused on arid and hyper arid region. But in the new concept of desertification as mentioned before as a "degradation process", it also happen in humid and sub humid regions with a accelerating rate because of poor land use practice and overgrazing. Mapping desertification in this area however is difficult due to cloud cover, data unavailability and limited investment. Current desertification mapping techniques are developed for arid region and are inappropriate for sub-humid desertification, both in term of scale and ecosystem characterization. There is a need for new monitoring approach specific for sub-humid area which utilize readily available earth observation system in a cost effective solution.

The case study in this paper is conducted in Vietnam. Geographically, Viet Nam is not designated as an arid or semi-arid country, however, some regions within the country are at risk from desertification. It is estimated that 9.34 million hectares of land in Viet Nam are degraded, and a substantial part of that is prone to desertification. Over the past 10 years, drought has caused severe impacts upon the agricultural and forestry production in many areas, especially in the central highland and coastal area of Viet Nam (UNCCD, 2002). In the coastal area long dry seasons together with short heavy rainfall in the rainy season have led to the following types of degradation:

- Moving sand due to strong wind along the coastal area.
- Salinization in sandy soil, formation of salt crust on soil surface.
- Water erosion due to deforestation and overgrazing.

The net result of such land degradation is significant disturbance of ecosystems with loss of biological and economical productivity. Mapping and monitoring of degradation processes are thus essential for drafting and implementing a rational development plan for sustained use of semi-arid land resources of Vietnam. The specific objectives of this study are: (1) to develop a operational methods for desertification mapping specific for semi-arid and sub-humid areas which combine the advantages of several types of readily available satellite imagery; (2) To test the new desertification mapping method as a quantitative assessment in the coastal areas of Vietnam.

STUDY AREA

The study area is located in Binh Thuan province, in south central Vietnam. The area faces the Pacific Ocean to the east with a coastline of 192 km (Fig. 1). The Truong Son mountain range, running from North-east to South-west, block most of the rain coming from the Thailand's sea, thus created semi arid conditions for the area.

Binh Thuan province can be divided into 4 main landscapes:

- Sand dunes along the coast (18.2% of total area).
- Alluvial plains (9.4% of total area).
- Hilly areas, with the average elevation of 50 m asl (31.6% of total area).
- The Truong Son mountain range (40.8% of total area).

Binh Thuan is the driest and hottest region of Vietnam. The climate is a combination of tropical monsoon and dry and windy weather. The mean annual temperature is 27°C, with average minimum 20.8°C in the coldest months (December, January), and an average maximum of 32.3°C in the hottest months (May and June). Binh Thuan also receives more solar radiation than any other area in Vietnam, with 2911 sunshine hour annually – or almost 8 hour per day.

Rainfall in this area is limited and irregular. Annual precipitation is 1024 mm, while evaporation in some years is equivalent to precipitation. At some locations annual rainfall can be as low as 550 mm. The dry season is from November to April, with 60 days of January and February having almost no rain. The rainy season is from May to October with heavy rain concentrated in a short periods with up to 200 mm/day.

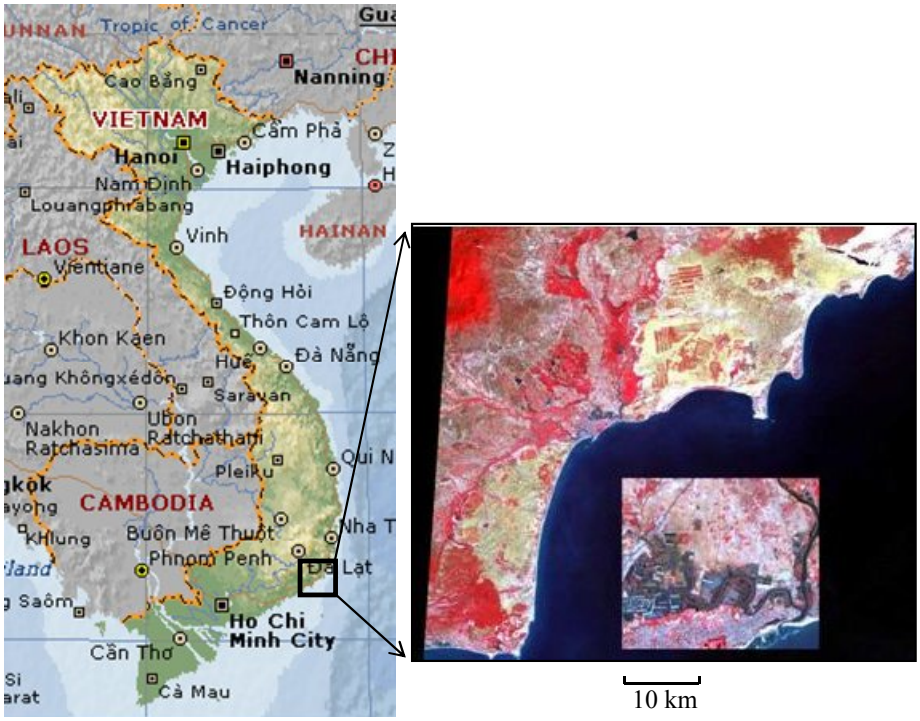

Figure 1. Location of study area. On the right is an ASTER image acquired on 22 Jan 2003 (band 321 in RGB). In the image red colours represent vegetated areas, white and yellow represent sandy soil.

DATA RESOURCES

1.2 Parameters required for desertification monitoring.

Desertification is a complex process which involves both natural factor and human activities. Depending on the level and nature of management, such as decision making, economic policy, and land use management, different kinds of information are required. DESERTLINKS (a European commission funded project) have listed 150 indicators for desertification assessment which involve ecological, economic, social and institutional indicators (Brandt et al., 2002). However, for desertification mapping three parameters are of

key importance – land surface temperature (LST), vegetation cover, and soil moisture. There have been several approaches adopted for desertification mapping. The first two are ground survey and image interpretation. Although different in scale and technique, both rely on expert knowledge and ability to visually analyse the landscape and group it to several predefined categories. The third, remote sensing based, approach is digital image classification based on a single image. The techniques and algorithms used can vary, but all are based on the spectral similarity of pixel values and a set of sample points with known characteristics. Class adjustment is based on local knowledge and ground observation.

The fourth approach is a group of techniques aiming at modelling the problem using physical parameters related to the land process, derived from Earth Observation data. Using geophysical parameters it is possible to assess the problem as it happens, and produce results that are comparable between different geographic regions. As mentioned above there are many indicators that can be used for desertification mapping, but not all are available or appropriate. However, in remote sensing we always need to generalize the problem to a few important factors that matter the most. To standardize the mapping method we develop a desertification index based on 3 parameters which strongly reflect the changes in desertification environment. These parameters are: land surface temperature (LST); vegetation cover; and soil moisture.

Satellite-derive land surface temperature (LST) has a strong relationship with the thermal dynamic of land processes (Dash et al., 2002), and can be use to assist is assessment of vegetation condition. In dry conditions high leaf temperatures are a good indicator of plant moisture stress and precede the onset of drought (McVicar, 1998), and surface temperature can rise rapidly with water stress and reflect seasonal changes in vegetation cover and soil moisture (Goetz, 1997).

In arid conditions vegetation provides protection against degradation processes such as wind and water erosion. Vegetation reflects the hydrological and climate variation of the dry ecology. Decreasing vegetation cover, and changes in the species composition of vegetation are sensitive indicators of land degradation (Haboudane et al., 2002).

Soil moisture is an important variable in land surface hydrological processes such as infiltration, evaporation and runoff; and is controlled by complex interactions involving soil, plant and climate (Puma et al., 2005). In arid and semi-arid areas, soil moisture can be use to monitor drought patterns and water availability for plant growth (Hymer et al., 2000). In an integrated mapping method, soil moisture can compensate for the weakness of vegetation indices in areas of sparse vegetation cover (Saatchi, 1994).

1.3 Remote Sensing data resources

Currently, medium spatial resolution sensors offer data with spatial resolution higher than 1 km. The sensors such as GLI, MODIS and MERIS can be considered as the next generation of NOAA AVHRR or SPOT VGT, offering multiple scale data (250 - 1000 m), improved spectral resolution (more band, better atmospheric calibration), and improved radiometric accuracy. At this resolution, a single scene can cover the entire coastal area of Vietnam. Some of the new high spatial resolution sensors are also listed in Table 1. This group of sensors provides multispectral imagery with resolutions between 5 and 100 m.

Table 1. Currently operational high spatial resolution multi-spectral sensors

Platform	LANDSAT 7	SPOT	EO-1	TERRA
Instrument	ETM+	HRG	ALI	ASTER
Resolution	15 to 120 m	10 to 20 m	10 to 30 m	15 to 90 m
Wavelength	PAN, SWIR, TIR	PAN, VNIR	VNIR, SWIR	VNIR, SWIR, TIR
Number of channels	7/8,	4	10	14
Swath width	185 km	60 km	37 km	60 km
Agency	NASA	SPOTIMAGE	NASA	NASA
Price ($/km^2)	0.018 – 0.158	0.67 – 1.43	Non-commercial	Non-commercial

Another sensor technology that is important to desertification monitoring is Synthetic Aperture Radar (SAR). The all-weather capability of spaceborne SAR sensors (

Table 2) is a major advantage over optical systems. SAR data can be used to estimate soil moisture content, which is an important parameter in semi-arid land where vegetation growth is heavily dependent on water availability (Karnieli *et al.*, 2002; Moran *et al*., 1998; Tansey and Millington, 2001; Wang *et al*., 2004).

Table 2. Currently operated SAR sensors

Platform	ERS-1/2	ENVISAT	Radarsat-1/2/3	JERS-1
Instrument	SAR	ASAR	SAR	SAR
Resolution	25 m	30-150 m	30-150 m	25 m
Frequency	C	C	C	L
Polarisation	VV	HH/HV	HH/VV/HV/VH	HH
Swath	100 km	50-500 km	10-500 km	75 km
Agency	ESA	ESA	CSA	NASDA

1.3.1 Specific requirements

In the context of the case study, suitable remote sensing data sources are sensors which could provide all or some of the parameters discussed in section 3.1. It is important to note that the "value" of each sensor is not only dependent on high spatial resolution, but also the spectral resolution, cost, coverage, calibration standards, and availability. Desertification is a long-term process, so an operational desertification monitoring system must be based on a robust and reliable suite of satellite sensors that can guarantee data continuity, quality, and availability on a decadal scale. It is for these reasons that only sensors from government-supported non-commercial Earth Observation programmes were considered for this project. Another issue that needs to be considered is data cost. As most desertification occurs in developing countries, a relatively low cost monitoring solution is required.

The high spatial resolution sensor selected for this project was ASTER. ASTER offers several advantages over rival sensors. It provides more bands in SWIR and TIR (6 bands in SWIR and 5 bands in TIR) than Landsat 7 ETM+ while retaining adequate spatial resolution in visible bands. The 5 TIR bands offer a more precise measurement of land surface temperature with an accuracy of 0.3^{o}C (Wan, 1999). Cost is an issue, with ASTER level 2 products available free of charge, while level 1 cost £50 per scene.

For radar imagery, we chose ENVISAT ASAR (Advance Synthetic Aperture Radar). ASAR provides multiple swath-widths with spatial resolutions ranging from 30 to 150 m. Thus it can be used for both national and local scale. Another advantage of ASAR is that the ENVISAT satellite also carries the MERIS sensor which can offer optical data acquisition simultaneously with SAR data.

A key feature of all the data sources listed above is the availability of standardised product formats and rigorous calibration, important for the development of long term quantitative monitoring.

1.3.2 RS data acquired

During the study period two sets of remote sensing data were collected representing dry season and wet season conditions. The dataset (Table 3) was successfully acquired in January 2005.

Table 3. Image acquisition

Date of acquisition	Sensor	Level/ Image mode
19 Jan 2005	ENVISAT ASAR	Level 2B/ ASAR IMG
19 Jan 2005	ENVISAT ASAR	Level 2B/ ASAR IMP
14 Jan 2005	ASTER	Level 1B/ AST_1B
14 Jan 2005	ASTER	Level 2/ ASTER_08
25 Oct 2005	ASTER	Level 1B/ AST_1B
25 Oct 2005	ASTER	Level 2/ ASTER_08
28 Oct 2005	ENVISAT ASAR	Level 2B/ ASAR IMG
28 Oct 2005	ENVISAT ASAR	Level 2B/ ASAR IMP

1.4 Other data sources

The following ancillary data are available:
- Topographic maps in digital format at 1:50,000 scale, with contour interval of 20 m.
- Land cover map for the year 2000 at 1:50,000 scale.
- Soil map at scale 1:1,000,000.
- Climate data from 1995 to 2004.

Two fieldwork visits were conducted in dry and wet seasons 2005, to provide the ancillary data and basic soil properties needed to validate the image processing result.

METHODS

1.5 Image pre-processing

For ASTER imagery, we used level 2 data which were atmospherically corrected at the data centre using a radiative transfer model and atmospheric parameters derived from the National Center for Environmental Prediction (NCEP) data (Abrams, 2000). ASTER images were registered to topographic map using second order transformation with sub-pixel RMS and nearest neighbourhood resampling.

For ENVISAT ASAR imagery, first we applied a Lee filter to remove the noise, then carried out an image-to image geometric correction using the previously georeferenced ASTER imagery. Raw ASAR image amplitude values were converted to backscatter using the equation provided by ESA (ESA, 2004).

$$\delta^0_{i,j} = \frac{DN^2_{i,j}}{K}\sin(\alpha_{i,j}) \qquad \textbf{(Equation 1)}$$

For i = 1…L and j= 1…M

Where K = absolute calibration constant

$DN^2_{i,j}$ = pixel intensity value at image line and column "i,j"

$\delta^0_{i,j}$ = sigma nought at image line and column "i,j"

$(\alpha_{i,j})$ = incident angle at image line and column "i,j"

Corrections for the effect of slope on local incident angle were applied to all SAR backscatter imagery using a slope map derived from the 1:50,000 digital topographic maps. The correction involved multiplying backscatter values by the ratio of backscatter received from a sloping surface to that received from a horizontal surface, where

$$\delta_s^0 / \delta_h^0 = \sin\Theta_i / \sin(\Theta_i - \Theta_{loc}) \quad \textbf{(Equation 2)}$$

δ_s^0 backscatter from sloping surface;

δ_h^0 backscatter from a horizontal surface;

Θ_i average radar incident angle

Θ_{loc} local incident angle determined from elevation model

The correction effect was minor in most cases because the study sites were mostly flat.

1.5.1 Land surface temperature (LST)

LST is retrieved from ASTER level_2 product, AST_08 surface kinetic temperature. This product has a spatial resolution of 90 m and is generated from the ASTER thermal bands using the TES algorithm (Gillespie et al., 1998). The product has been validated to an accuracy of 1K degree under clear sky condition (Wan, 1999).

1.5.2 Vegetation Index

Vegetation cover was estimated from ASTER imagery using NDVI and SAVI (Soil Adjusted Vegetation Index). SAVI is a modification of NDVI with an L factor to compensate for vegetation density. Several author recommend SAVI for sparsely vegetated areas (e.g. Huete, 1998; Terrill, 1994).

$$SAVI = \frac{NIR - RED}{NIR + RED + L}(1 + L) \quad \textbf{(Equation 3)}$$

1.5.3 Soil moisture estimation

In this study we applied the data fusion approach proposed by (Sano, 1997) , in which the effects of soil roughness are accounted for by differencing the SAR backscatter from a given image and the backscatter from a "dry season" image (σ^o-$\sigma_{dry}{}^o$). The vegetation influence was corrected by using an empirical relationship between σ^o-$\sigma_{dry}{}^o$ and the vegetation index.

Sano (1997) found that the vertical distance between a given point and the line defining the (σ^o-$\sigma_{dry}{}^o$)/Green Leaf Area Index (GLAI) relation was independent of surface roughness and vegetation density, and directly related to target's surface soil moisture content. It is important to note that a given relationship, as illustrated in Fig. 2, would be valid only for a single SAR configuration (i.e. sensor polarization and frequency) and would need to be adjusted for the influence of topography on local incidence angle. This, however, should not be an issue for this study, as majority of land in the test site is relatively flat.

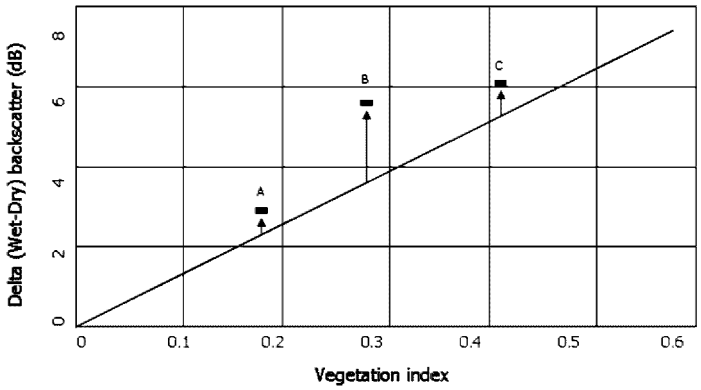

Figure 2. A graphic illustration of the SAR/optical approach for evaluating surface soil moisture developed by (Sano, 1997). The vertical distance of points A–C from the solid line is related directly to soil moisture content.

To normalize the difference between pixel values and the corresponding dry scene values, a delta index was proposed by *(D.P. Thoma et al., 2006)*. The delta index represents a change relative to dry scene backscatter, and thus the delta index should be interpreted in light of dry scene soil moisture. This is because any dry scene backscatter is likely to be affected by at least a small amount of residual soil moisture.

$$\textbf{Delta index} = \left| \frac{\delta^0_{wet} - \delta^0_{dry}}{\delta^0_{dry}} \right| \quad \textbf{(Equation 4)}$$

Where δ^0_{dry} = backscatter from a pixel in dry season

δ^0_{wet} = backscatter from the same pixel in wet season

1.5.4 Vegetation Temperature Condition Index (VTCI)

VTCI was developed by Wan et al. (2004) and is defined as the ratio of LST differences among pixels with a specific NDVI value in a sufficiently large area; the numerator is the difference between maximum LST of the pixels and LST of one pixel; the denominator is the difference between maximum and minimum LST of the pixels.

$$VTCI = (LST_{NDVIi.max} - LST_{NDVIi}) / (LST_{NDVIi.max} - LST_{NDVIi.min}) \quad \textbf{(Equation 5)}$$

where:

$$LST_{NDVIi.max} = a + b\ NDVI_i$$
$$LST_{NDVIi.min} = a' + b'\ NDVI_i \quad \textbf{(Equation 6)}$$

where $LST_{NDVIi.max}$ and $LST_{NDVIi.min}$ are maximum and minimum LSTs of pixels which have same $NDVI_i$ value in a study region, and LST_{NDVIi} denotes LST of one pixels whose NDVI value is $NDVI_i$. Coefficients a, b, a', and b' can be estimated from an area large enough where soil moisture at surface layer should span from wilting point to field capacity at pixel level. In practice, the coefficients are estimated from a scatter plot of LST and NDVI in the study area.

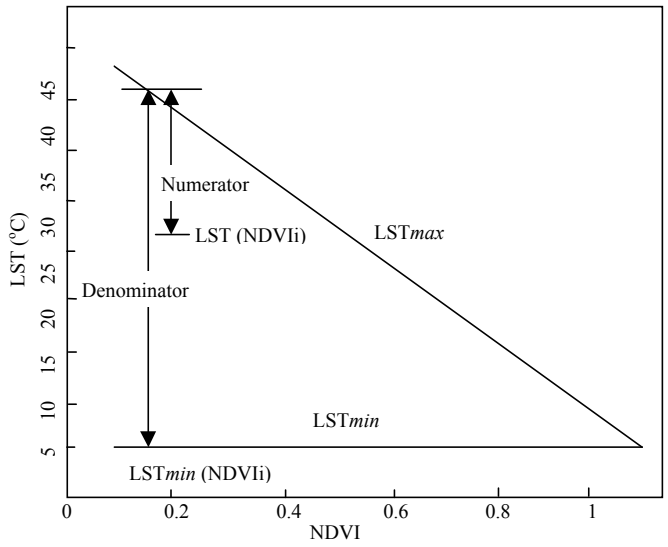

Figure 3. Schematic plot of the physical interpretation of VTCI (adapted from Wan et al. 2004)

VTCI can explain both the changes of vegetation in the region and the thermal dynamics of pixels that have the same vegetation density. It can be physically explained as the ratio of temperature differences among pixels (Fig. 3). The numerator of equation (4) is the difference between maximum LST of pixels with the same NDVI value and LST of one pixel, while the denominator is the difference between maximum and minimum LST of the pixels. In figure 2, LST_{max} can be regarded as 'warm edge' where there is less soil moisture availability and plants are under dry condition; LST_{min} can be regarded as the 'cold edge' where there is no water restriction for plan growth (Gillespie *et at*. 1997, Wang *et al*. 2004). The value of VTCI ranges from 0 to 1; the lower the value of VTCI, the closer a pixel to the warm edge and the higher the occurrence of drought and water stress.

1.6 Field methodologies

Two field surveys (dry and wet season) are required in order to gather the necessary field observations. The first field visit was conducted in January-February 2005 (dry season). 150 sample locations were selected using a stratified random sampling method. This method is preferred over full random sampling because stratified sampling allowed us to distribute sample plots over the entire range of land use/land cover types without bias (Congalton, 1991; Stehman, 1999).

Stratification was based on unsupervised classification of a January 2003 ASTER image. The classification results provided a general guide to the location, size and type of desertification. Seven land cover classes were generated by unsupervised classification, which corresponded to high sand dune, low sand dune, bare sandy soil, rice field, grazing land, scattered forest on low land, and dense forest on hilly area.

At each sample point the following parameters were measured:

- vegetation type & cover %
- Top soil texture (5 cm depth)
- pH, EC
- Surface roughness: measured in the field with paper profile
- Soil moisture (0-10 cm, and 10-20 cm).
- Soil surface temperature

RESULTS

1.7 Vegetation condition index

NDVI is calculated from band 3 and band 1 while LST is readily available from AST_08 product as mentioned in section 1.5.1. To reduce the error in spatial resolution differences, NDVI imagery was resampled from 15 m to 90 m, to give the same pixel size as the thermal band. Figure 4 is the scatter plot of LST and NDVI of the study area. The straight lines drawn on the scatter plot represent the 'warm edge' (LST_{max}), and the lower limits of the scatter plot represent the 'cold edge' (LST_{min}).

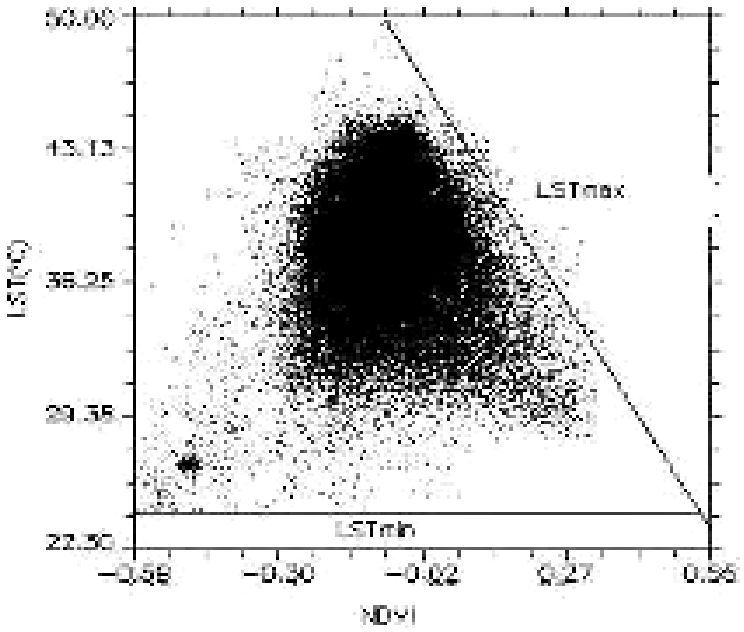

Figure 4. Scatter plot of LST versus NDVI (ASTER image 16 June 2005).

From the 'warm edge' and 'cold edge' we get the coefficients a, b, a', b':

$$LST_{NDVIi.max} = 43.3 - 29.75(N$$
$$LST_{NDVIi.min} = 25.2 + 0(NDVI$$ **(Equation 7)**

Using (Equation 7) and **(**Equation 5), we get the VTCI image of the study area for both dry and wet season. We can see that bare sandy soil areas have low VITC values in both dry and wet season which implies drought and water stress. The sandy soil area has a lighter tone in Figure 5 (a) and (b). Sand dunes along the coastal area, show unexpected results, having a relatively higher VTCI, from which it might be wrongly interpreted that the area was not suffering from water stress. This can be explained by the fact that the sand dune area is pure sand with no significant vegetation cover. A drought index based on vegetation stress will thus indicate low stress values for this area. Indices such as the VTCI should be interpreted with caution, and not used for areas of sparse vegetation. In the feature space of LST and NDVI (Figure 3), for the same temperature, if NDVI decreases VTCI will increase. On the other hand, for areas with the same NDVI, the higher the temperature, the higher level of vegetation stress, because there is less water left on the soil for plant transpiration.

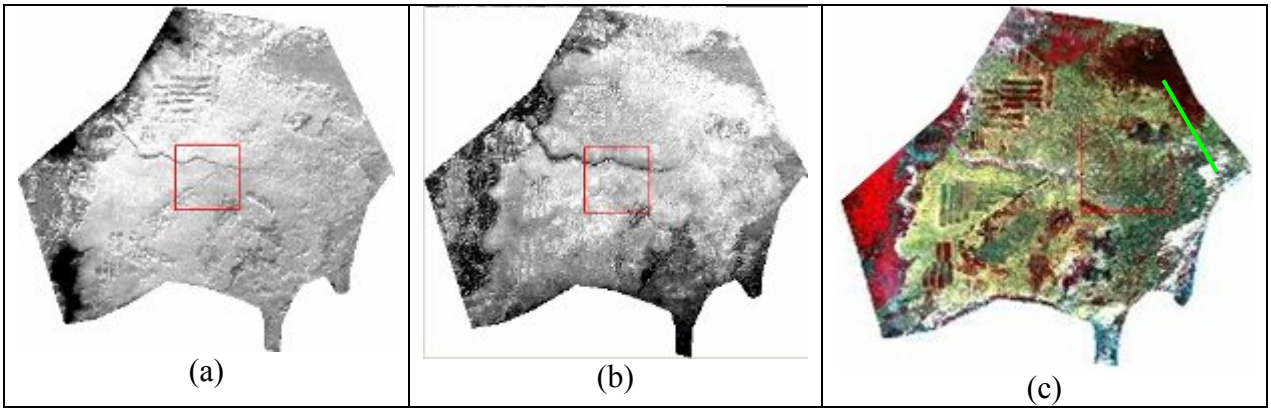

Figure 5. VTCI and colour composite of the study area: (a) VTCI wet season, (b) VTCI dry season, (c) ASTER false colour composite (band 321 in RGB). Green line the left of colour composite show position of the transact in Figure 6

To investigate how VTCI changes between dry and wet seasons, a 5 km transect was positioned crossing 3 types of land cover: sand dune, sandy soil and dry open forest. In general VTCI values from the wet season have higher values than the dry season, which reflects the overall change in water availability and a healthier vegetation condition. In the sand dune area (a), however, the changes between two seasons are small because of its low ability to retain rain water in the surface layers and lack of vegetation. The flat sandy soil area (b) exhibits a large change in VTCI between the two seasons, clearly showing the effect of rainfall which boosts the vegetation growth. The sandy soil area also shows a broad range of variation in both seasons with bare soil having VTCI values as low as 0.1 and vegetated land have VTCI values as high as 0.28 in the dry season.

The open dry forest has a higher VTCI than sandy soil in the wet season due to its ability to retain moisture and the high photosynthesis activity. In the dry season, the open dry forest loses all of its leaves, opens its canopy and becomes very dry, which is reflected in a VTCI as low as bare sandy soil.

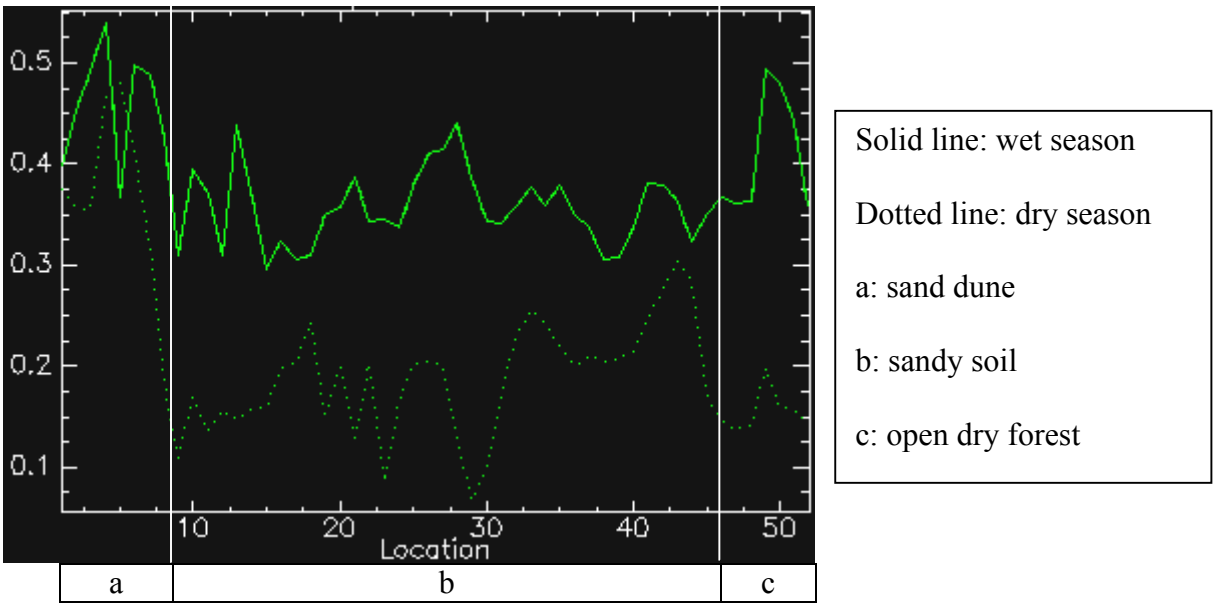

Figure 6. VTCI profile from dry at wet season. (see Figure 5 for position on image)

1.8 Soil moisture estimation

The relationship between delta index and soil moisture is determined by soil dielectric properties. These are the dependency of dielectric constant on volumetric soil moisture, and the dependency of backscatter on real dielectric constant. The lower the dielectric constant, the more incident energy is absorbed, giving a lower backscatter value. In addition, radar backscatter is also affected by topography, surface roughness and vegetation cover. By taking the delta index we could remove those time-invariant features because they are the same in dry/wet season imagery. The difference in image backscatter between seasons should be due primarily to soil moisture.

The results showed that, for the whole area, delta index backscatter were poorly correlated (r^2= 0.58) with soil moisture content (Figure 7). This poor correlation could be attributed to the change in vegetation between dry and wet season as discussed earlier in section 1.7

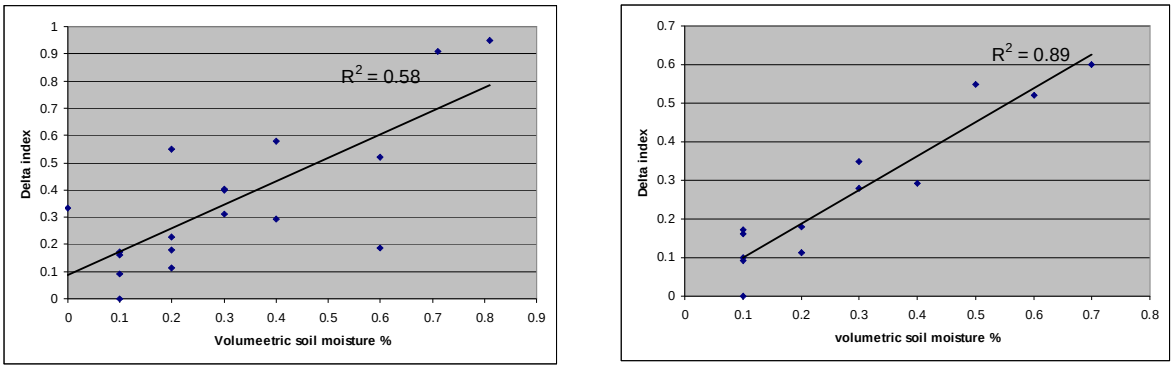

(a) (b)

Figure 7. The relation between delta index backscatter and surface soil moisture: (a) all areas; (b) sandy soil and bare land area

Considering only the sandy soil and bare land area, there was a strong relation between delta backscatter and soil moisture (R^2= 0.89). Using this relationship, a regional map of surface soil moisture was obtained for the 2005 wet season. The map showed a good contrast among sand dunes along the coast (green), sandy soil (red) and rice fields (yellow). Several black areas in the middle of image are lakes which have very low backscatter in both seasons. Forest areas (SAVI >0.4) were misinterpreted as having very low soil moisture (green area apart from sand dune along the coast) because the delta index model performs poorly in heavily vegetated areas.

Although the delta index does not yield a 1:1 relationship with soil moisture, the map provides a reasonable estimation of soil moisture, at least for sandy soil areas.

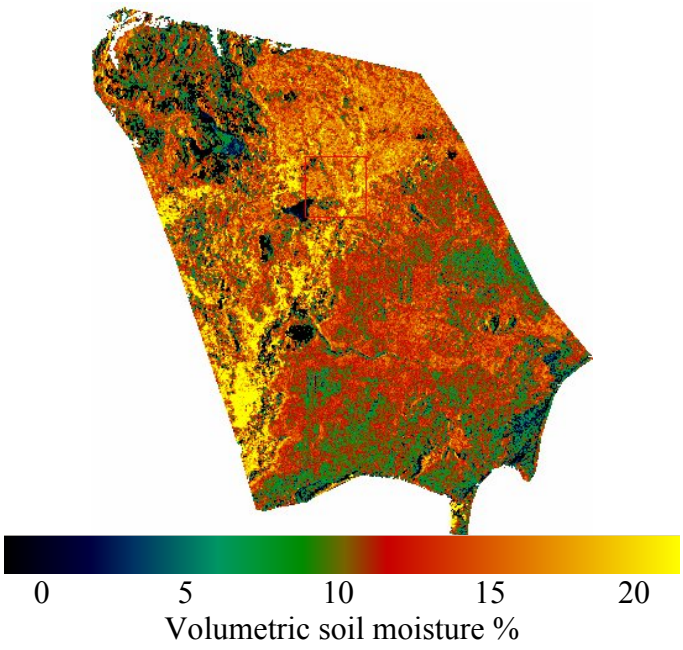

Figure 8. Regional map of surface soil moisture based on delta index. Wet season 2005

DISCUSSION

The results of the initial analysis have shown that standard ASTER image products have strong potential for desertification mapping at medium scales, clearly delineating the coastal sand dune, sandy soil, agriculture and vegetated areas.

VTCI calculated from two seasons of ASTER data have shown that the index can provide quantitative information on spatial and temporal changes caused by the desertification process. Time series of VTCI have the potential to detect not only areas with water stress problems but also areas which are stable over the time. This information is a valuable input for land use planning strategies that are aimed at combating desertification.

The preliminary results of soil moisture estimation from SAR delta index backscatter are encouraging. If NDVI values are less than 0.4 we can use delta index to estimate soil moisture, as has been demonstrated for sandy soil areas (r^2=0.89). For vegetated areas (NDVI >0.4), SAR backscatter is less successful at model soil moisture due to the influence of the canopy.

Soil moisture estimation when combined with VTCI and others parameters will provide a better view of desertification process. While delta index works well for open sandy soil, VTCI can provide accurate information for vegetated area. Integration of parameters extracted from different parts of the spectrum or different sensors gives more information on different aspects of the desertification process, therefore improve the mapping accuracy.

REFERENCES

Abrams, M., 2000. The Advanced Spaceborne Thermal Emission and Reflection Radiometer (ASTER): Data products for the high spatial resolution imager on NASA's Terra platform. International Journal of Remote Sensing, 21(5): 847-859.

Brandt, J., Geeson, N. and Imeson, A., 2002. A desertification indicator system for Mediterranean Europe. DesertLink.

Congalton, R.G., 1991. A review of assessing the accuracy of classification of remotely sensed data. Remote Sensing of Environment, 37: 35-46.
D.P. Thoma, M.S. Moran, R. Bryant and Rahman, M., 2006. Comparision of four models to determine surface soil moisture from C-band radar imagery in a sparsely vegetationed semiarid landscape. Water resources research, 32: 1-12.
Dash, P., Tsche, F.M.G., OLESEN, F.S. and FISCHER, H., 2002. Land surface temperature and emissivity estimation from passive sensor data: theory and practice–current trends. International Journal of Remote Sensing, 23(13): 2563–2594.
Dwivedi, R.S., Sankar, T.R., Venkataratnam, L. and Rao, D.P., 1993. Detection and delineation of various desert terrain features using Landsat-TM derived image transforms. Journal of Arid Environments, 25(1 SU -): 151-162.
ESA, 2004. ENVISAT ASAR product handbook. Europen Space Agency (ESA).
Gillespie, A. et al., 1998. A temperature and emissivity separation algorithm for Advanced Spaceborne Thermal Emission and Reflection Radiometer (ASTER) images. IEEE Transactions on Geoscience and Remote Sensing, 36(4): 1113 - 1126.
Goetz, S.J., 1997. Multi-sensor analysis of NDVI, surface temperature and biophysical variables at a mixed grassland site. International Journal of Remote Sensing, 18: 71-94.
Grainger, A., 1990. The Threatening desert - controlling desertification. Earth Scan, London, 369 pp.
Haboudane, D., Bonn, F. and Royer, A., 2002. Land degradation and erosion risk mapping by fusion of spectrallybased information and digital geomorphometric attributes. International Journal of Remote Sensing, 23(18): 3795–3820.
Hymer, D.C., Moran, M.S. and Keefer, T.O., 2000. Soil water evaluation using a hydrologic model and calibrated sensor network. Soil Science Society of America Journal, 64(1): 319-326.
Karnieli, A., Gabai, A., ICHOKU, C., ZAADY, E. and SHACHAK, M., 2002. Temporal dynamics of soil and vegetation spectral responses in a semi-arid environment. International Journal of Remote Sensing, 23(19): 4073–4087.
McVicar, T.R., Jupp, D.L.B., 1998. The current and potential operational use of remote sensing to aid decisions on drought exceptional circumstances in Australia: a review. Agricultural Systems, 57: 399-468.
Mering, C., Poncet, Y., Jacqueminet, C. and Rakoto-Ravalontsalama, M., 1987. Quantitative description of denudation forms in the Western African Sahel. Advances in Space Research, 7(3 SU -): 31-39.
Moran, M.S., Daniel, C.M. and Jiaguo Qi, 1998. Soil moisture evaluation using radar and optical remote sensing in semearid rangeland. Semi-Arid Land-Surface-Atmosphere (SALSA) Program.
Puma, M.J., Celia, M.A., Rodriguez-Iturbe, I. and Guswa, A.J., 2005. Functional relationship to describe temporal statistics of soil moisture averaged over different depths. Advances in Water Resources, 28(6): 553-566.
Rebillard, P., Pascaud, P.N. and Sarrat, D., 1984. Merging Landsat and spaceborne radar data over Tunisia. Advances in Space Research, 4(11 SU -): 133-138.
Robinove, C.J., Chavez, J., Pat S., Gehring, D. and Holmgren, R., 1981. Arid land monitoring using Landsat albedo difference images*1. Remote Sensing of Environment, 11 SU -: 133-156.
Saatchi, S.S., Moghaddam, M., 1994. Biomass distribution in boreal forest using SAR imagery, Multispectral and Microwave Sensing of Forestry, Hydrology, and Natural Resources. The International Society for Optical Engeneering, Rome, Italia, pp. 437-448.

Sano, E.E., Qi, J., Huete, A.R., Moran, M.S., 1997. Sensitivity analysis of C and K band synthetic aperture radar data to soil moisture content in semiarid regions. Ph.D.Dissertation, University of Arizona,, Tucson, 122 pp.
Stehman, S.V., 1999. Basic probability sampling designs for thematic map accuracy assessment. International Journal of Remote Sensing, 20(12): 2423-2441.
Tansey, K.J. and Millington, A.C., 2001. Investigating the potential for soil moisture and surface roughness monitoring in drylands using ERS SAR data. International Journal of Remote Sensing, 22(11): 2129–2149.
Tucker, C.J., 1980. A critical review of remote sensing and other methos for non-destrictive estimation of standing crop biomass. Grass and Rorage Science, 35: 115-182.
Tucker, C.J., 1987. Sattellite remote sensing of drough conditions. Remote sensing of Environment, 23: 243-251.
UN, 2003. Fact Sheets on the Convention to Combat Desertification. United Nations.
UNCCD, 2002. Vietnam report on the UNCCD implementation. UNCCD.
UNCCD, 2004. UNCCD 10 years on. United Nation.
Wan, Z., 1999. MODIS Land-Surface Temperature Algorithm Theoretical Basis Document. Institute for Computational Earth System Science. University of California, Santa Barbara.
Wang, C., Qi, J., Moran, S. and Marsett, R., 2004. Soil moisture estimation in a semiarid rangeland using ERS-2 and TM imagery. Remote Sensing of Environment, 90(2): 178-189.